



HAL
open science

Ships hull corrosion diagnosis from close measurements of electric potential in the water

A. Guibert, O. Chadebec, J.-L. Coulomb, Corine Rannou, R. P. P Nogueira

► **To cite this version:**

A. Guibert, O. Chadebec, J.-L. Coulomb, Corine Rannou, R. P. P Nogueira. Ships hull corrosion diagnosis from close measurements of electric potential in the water. *European Physical Journal: Applied Physics*, 2010, 52 (2), 10.1051/epjap/2010145 . hal-00634370v2

HAL Id: hal-00634370

<https://hal.science/hal-00634370v2>

Submitted on 26 Nov 2020

HAL is a multi-disciplinary open access archive for the deposit and dissemination of scientific research documents, whether they are published or not. The documents may come from teaching and research institutions in France or abroad, or from public or private research centers.

L'archive ouverte pluridisciplinaire **HAL**, est destinée au dépôt et à la diffusion de documents scientifiques de niveau recherche, publiés ou non, émanant des établissements d'enseignement et de recherche français ou étrangers, des laboratoires publics ou privés.

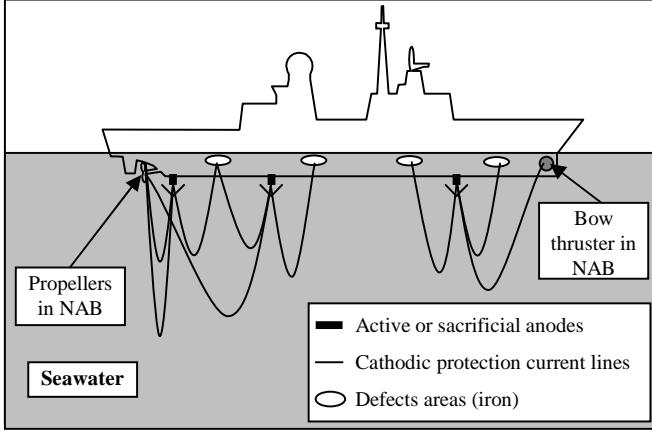


Fig. 2. Cathodic protection current lines spreading in the seawater, under the ship. They go back to the hull through the defects and the noble areas.

It is important to see that with both cathodic protections, the current goes back to the structure through the damaged areas (cathodes). If it was possible to perform many electric potential (or current) measurements stuck to the structure, it would be easy to find the corroded areas: it would be the areas where currents go back to the hull or the ones with the less electric potentials. But in practice a user does not have the time to get so many measurements and cannot do them so close to the structure.

The purpose of this article is to show the possibility of such a diagnosis with a limited number of measurements, not so close to the structure. Some kind of studies have been made [1] [2] but in internal problems. The structure here can be a pipe line or any piece of painted steel fully drowned in the seawater. The conduction is then not bounded and the problem is called external.

First the forward modeling of this phenomenon will be presented: this means providing an electromagnetic prediction from the knowledge of some boundary conditions on the structure. Then an inverse method will be extrapolated to make a diagnosis. This means to find the boundary conditions of the structure (and so the corroded areas) from a series of electromagnetic measurements. Finally some experimental results will be presented to corroborate the method.

The example taken in the whole article will be a ship hull protected with an ICCP, but the extrapolation to get the case of SACP will be often reminded.

2 PREDICTION: THE FORWARD MODELING

As mentioned above, the considered case here will be a piece of painted steel equipped with defects and an ICCP, drowned in an infinite electrolyte; this means far from the sea floor and from the surface (also previously called external problem). It is also possible to consider the sea floor and surface (to model the immersed part of a floating vessel for example), then the problem becomes internal. This last case will be considered in the experimentation part.

The piece of steel shape studied is a ship mock-up with defects and ICCP protection on its lowest parts. Numerical simulations have shown that placing ICCP and defects there

impose currents lines spreading under the steel. In this case, modeling the water surface is not useful: The infinite problem described can also be semi infinite. In this way, all the simulations made further in the article (in an infinite domain with the mock-up) are representative of the immersed part of a ship far away from the sea floor.

To examine such an external problem, it is necessary to think about the modeling method to use. First, the method has to easily take into account the infinite bound, case often faced. But as developing an inverse method is the main goal of the study, the method has to create a system linking directly the boundary conditions. The Boundary Elements Method (often called BEM) has both advantages and will be chosen for the study [3].

2.1 Governing equations and BEM method

The problem exposed above deals with some current injection in the resistive seawater which comes back to the hull through the defects. This is a conduction problem, whose main unknown is then the electrical potential φ in the seawater defined by the Faraday law:

$$\mathbf{E} = -\mathbf{grad}(\varphi) \quad (1)$$

E is the electric field defined by:

$$\mathbf{J} = \sigma \mathbf{E} = -\sigma \mathbf{grad}(\varphi) \quad (2)$$

This also induces a very useful equation:

$$J_n = \mathbf{J} \cdot \mathbf{n} = \sigma \mathbf{E} \cdot \mathbf{n} = -\sigma \mathbf{grad}(\varphi) \cdot \mathbf{n} = -\sigma \frac{\partial \varphi}{\partial n} \quad (3)$$

The σ parameter is the seawater conductivity, related to its salinity. Moreover, the seawater will be supposed homogenous and isotropic, with non additional charges so that the Laplace equation is verified:

$$\Delta \varphi = 0 \quad (4)$$

Green's first identity gives:

$$\int_V (u \Delta v - v \Delta u) dV = \int_S (u (\partial v / \partial n) - v (\partial u / \partial n)) dS \quad (5)$$

Replacing u by the electric potential φ and v by Green's function in 3D:

$$G(M, P) = 1 / r_{PM} = 1 / |PM| \quad (6)$$

We obtain Green's 3rd identity, linking the potential and its normal derivative on the whole surface:

$$h(P) \cdot \varphi(P) = \int_S \varphi(M) (\partial G(M, P) / \partial n) dS - \int_S G(M, P) (\partial \varphi(M) / \partial n) dS \quad (7)$$

h coefficient is the solid angle the point P sees around. It is possible to extrapolate (4) for P on the boundaries of the problem (non singular ones i.e. P on a plane boundary) with the introduction of a potential for the infinity bound φ_∞ , (Fig.

3). Indeed, two choices remain for this infinity bound: to set the infinity bound potential or the current density. The choice made here is to set the current on the infinity bound to zero, letting an infinite potential φ_∞ exist [4]. This potential, taken as a reference potential will be then very useful during the resolution. The further potential results are then obtained regarding this reference. The Green 3rd identity on the boundaries of the problem becomes:

$$\begin{aligned} -2\pi\varphi(P) &= \int_S \varphi(M) \cdot (\partial G(M, P) / \partial n) dS \\ &- \int_S G(M, P) \cdot (\partial \varphi(M) / \partial n) dS - 4\pi\varphi_\infty \end{aligned} \quad (8)$$

The described problem can be illustrated by the following scheme:

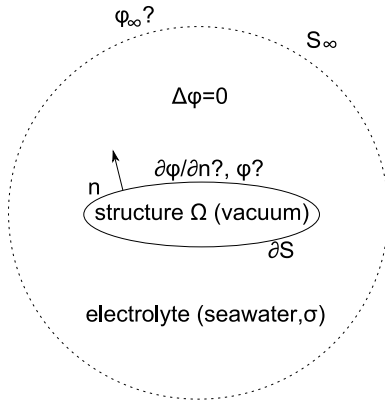


Fig. 3. Schematic representation of the boundary problem, a closed structure filled with air is drowned in an infinite domain. An infinite bound is represented to make the problem external.

Equation (5) is applied on the whole surface of the problem. The values of the unknowns vary on the entire model and the geometries studied are not simple. That is why it is impossible to compute analytically the integral term in (5) and the next step is to mesh the model.

In a first approximation an order 0 approach of the unknowns is made: all quantities are set constant on each element. The unknowns are then located at each elements barycenter: this is also called a point matching method. The error induced by this approximation is insignificant in our case, so more complicated modeling will not be exposed. Moreover, the measurements made hereinafter are not very close to the model: this explains why the approximation provides quite good results. Finally, this approximation avoids singularities on the further computations. After meshing, the system obtained is:

$$[H \quad T \quad -4\pi] \begin{bmatrix} \varphi \\ \partial \varphi / \partial n \\ \varphi_\infty \end{bmatrix} = 0 \quad (9)$$

The corresponding H and T equal to:

$$H_{ij} = - \int_{\Omega_j} \frac{\partial}{\partial n_M^{(j)}} \left(\frac{1}{r_{PM}^{(j)}} \right) dS_M^j = - \int_{\Omega_j} \frac{\vec{n}_M^{(j)} \cdot \vec{r}_{PM}^{(j)}}{(r_{PM}^{(j)})^3} dS_M^j \quad (10)$$

$$T_{ij} = \int_{\Omega_j} \frac{1}{r_{PM}^{(j)}} dS_M^j$$

Indeed the unknowns can be taken out of the integral term as they are considered constant on the integration surface (order 0). The first step of the system creation is to build the left matrix, containing all surface integrations computed at each barycenter. This part relatively complicated: analytically integrate would spend too much time so the solution chosen is to proceed to a numerical integration. The method used is the Gauss integration process. The integration term T becomes, for a sufficient number m of Gauss points:

$$T_{ij} = \int_{\Omega_j} \frac{1}{r_{PM}^{(j)}} dS_M^j \approx \sum_{q=1}^m \frac{1}{r_{PMq}^{(j)}} W_q \quad (11)$$

$r_{PMq}^{(j)}$ is the distance between the P point (where the integration is computed) and each Gauss point, W_q is the weight given to the q-Gauss point. The only variable to study is the number of Gauss points to place on the surface to get integrations close to the analytical ones. One difficulty comes from the choice of the number m of Gauss points: for an element P, the influence (i.e. the integration) of a far element is not preponderant and it needs only a few Gauss points but it is not the case of a neighbor element which needs many ones. A fixed number is not well optimized, but with simple geometries meshed uniformly, this will work quite well.

In our studies where geometries do not exceed one or two meters, and where meshing elements can reach 10 square centimeters, around 25 to 64 Gauss points are set. [3]

An important error occurs when computing numerically the influence of an element on itself. This error is erased by an analytic correction: the integral term in H_{ii} and T_{ii} are computed analytically.

As the integral computation is done, the separation of variable can be done. The boundary conditions available for an active protection (PCCI) are the active anode (A), the polarizable cathode (C) and the isolated part (I). The systems can be finally written:

$$\begin{bmatrix} H_{11} + 2\pi & H_{12} & H_{13} & T_{11} & T_{12} & T_{13} & -4\pi \\ H_{21} & H_{22} + 2\pi & H_{23} & T_{21} & T_{22} & T_{23} & -4\pi \\ H_{31} & H_{32} & H_{33} + 2\pi & T_{31} & T_{32} & T_{33} & -4\pi \\ 0 & 0 & 0 & A_1 & A_2 & A_3 & 0 \end{bmatrix} \begin{bmatrix} \varphi_A \\ \varphi_C \\ \varphi_I \\ \frac{\partial \varphi_A}{\partial n} \\ \frac{\partial \varphi_C}{\partial n} \\ \frac{\partial \varphi_I}{\partial n} \\ \varphi_\infty \end{bmatrix} = [0] \quad (12)$$

The A_i is the area of the element i. $\text{div}(\mathbf{J}) = 0$ is included in the Laplace equation (starting point of the system) but the introduction of φ_∞ does not ensure this equality anymore. The last line is then added to ensure this condition. It is interesting to remark in (9) that, if the problem is meshed in N elements, the system has N+1 equations for 2N+1 unknowns.

2.2 Application for a PCCI case

Since the problem studied here deals with PCCI, the boundary conditions physically mean:

- Anode regions (non-polarizable electrode), have their current density J_A known. $\partial\varphi_A/\partial n$ is linked to J_A by multiplying it by σ , the conductivity of the electrolyte.
- Cathode regions (polarizable electrode), have their polarization law $\partial\varphi_C/\partial n=f(\varphi_C)$ known and are most of the time non linear.
- On insulator regions the current density is null: $\partial\varphi_I/\partial n=0$.

The previous system (6) can then be written, by separating known and unknown variables:

$$\begin{bmatrix} H_{11}+2\pi & H_{12} & H_{13} & T_{12} & -4\pi \\ H_{21} & H_{22}+2\pi & H_{23} & T_{22} & -4\pi \\ H_{31} & H_{32} & H_{33}+2\pi & T_{32} & -4\pi \\ 0 & 0 & 0 & A_2 & 0 \end{bmatrix} \begin{bmatrix} \varphi_A \\ \varphi_C \\ \varphi_I \\ \frac{\partial\varphi_C}{\partial n} \\ \varphi_\infty \end{bmatrix} = \begin{bmatrix} -T_{11} \cdot \frac{\partial\varphi_A}{\partial n} \\ -T_{21} \cdot \frac{\partial\varphi_A}{\partial n} \\ -T_{31} \cdot \frac{\partial\varphi_A}{\partial n} \\ -A_1 \cdot \frac{\partial\varphi_A}{\partial n} \end{bmatrix} \quad (13)$$

The only information not used is the polarization law. Its non-linearity makes the resolution problematic:

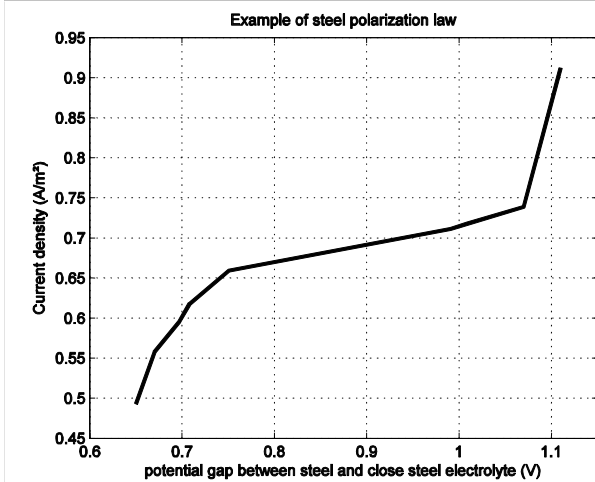


Fig. 4. Example of a non linear polarization law of steel. The steel is the reference in our problem so the abscissa scale is not a potential gap but only the electrolyte potential close to steel.

As said in the legend, the steel is the reference. The curve gives then the relation f between the current density received by the metal and its electric potential:

$$\left(\frac{\partial\varphi_C}{\partial n}\right)^{PL} = f(\varphi_C) \quad (14)$$

This knowledge simplifies the (13) system which can then be solved by an iterative solver; the one chosen is a Newton Raphson [5] algorithm. The varying parameter is φ_C , which is noted φ_C^{NR} below. The previous system becomes:

$$\begin{bmatrix} H_{11}+2\pi & H_{13} & T_{12} & -4\pi \\ H_{21} & H_{23} & T_{22} & -4\pi \\ H_{31} & H_{33}+2\pi & T_{32} & -4\pi \\ 0 & 0 & A_2 & 0 \end{bmatrix} \begin{bmatrix} \varphi_A \\ \varphi_I \\ \left(\frac{\partial\varphi_C}{\partial n}\right)^{BEM} \\ \varphi_\infty \end{bmatrix} = \begin{bmatrix} -H_{12} \cdot \varphi_C^{NR} - T_{11} \cdot \frac{\partial\varphi_A}{\partial n} \\ -(H_{22}+2\pi) \cdot \varphi_C^{NR} - T_{21} \cdot \frac{\partial\varphi_A}{\partial n} \\ -H_{32} \cdot \varphi_C^{NR} - T_{31} \cdot \frac{\partial\varphi_A}{\partial n} \\ -A_1 \cdot \frac{\partial\varphi_A}{\partial n} \end{bmatrix} \quad (15)$$

Considering the size of the left matrix, it is interesting to observe that if the problem has N meshing elements; this matrix has $N+1$ equations (lines) and $N+1$ unknowns (rows). The new system is square and can be easily solved.

In the Newton Raphson algorithm, the residual norm to minimize is the difference between the $\partial\varphi_C/\partial n$ obtained with the system (9) and the one got with the polarization law:

$$R(\varphi_C) = \left(\frac{\partial\varphi_C}{\partial n}\right)^{BEM} - \left(\frac{\partial\varphi_C}{\partial n}\right)^{PL} = \left(\frac{\partial\varphi_C}{\partial n}\right)^{BEM} - f(\varphi_C) \quad (16)$$

The two quantities $(\partial\varphi_C/\partial n)^{BEM}$ and $f(\varphi_C)$ can be computed from the knowledge of φ_C . The Newton Raphson algorithm makes the φ_C parameter vary to minimize the residual. When the algorithm has correctly converged, the two $(\partial\varphi_C/\partial n)$ are close to equality and the solution obtained has a physical behavior.

With a good starting point for the algorithm (often situated at the middle of the polarization law), the system converges in less than a dozen iterations. It is possible to insert the infinite potential in the varying parameters, adding a new line in the residual norm system ($\text{div}(\mathbf{J})=0$ again), which makes the algorithm numerically converge faster: in 3 to 6 iterations. The accuracy of the algorithm's convergence does not have to be very low, as the quantities $\partial\varphi_C/\partial n$ have values close to the unit. For example, in the further cases, a precision of 10^{-4} is in most of times sufficient.

One example of resolution is shown below with a ship hull model under cathodic protection (ICCP) meshed in 1052 elements:

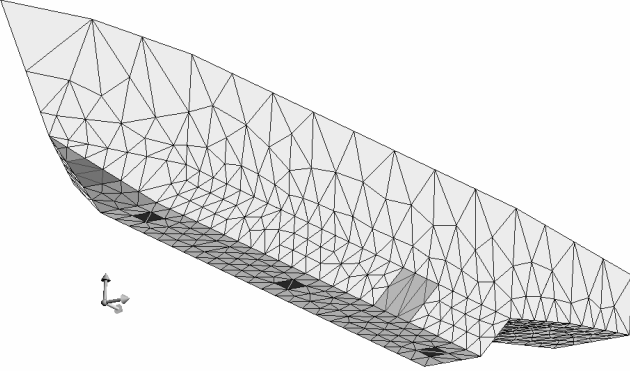


Fig. 5. Geometry meshed of an existing mock-up with: 3 uniform active anodes under the hull (6 elements in black), 4 different cathodes (31 elements in grey), and the hull completely isolated (1015 elements in white)

The algorithm presented above is used to compute the boundary conditions on the whole surface. The results are presented in the following Fig. 5:

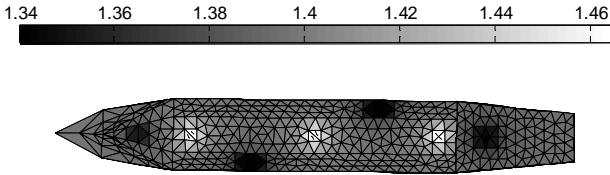


Fig. 6. Boundary conditions (electric potential and current densities) obtained on the hull with $\varphi_\infty = 1.3762$ V. The scale is in volts

The scale of the figure is in volts and the values are centered on the infinite potential. The white areas correspond to the active anodes and, as said in the introduction, they have the higher potential. The paint defects are colored in dark and as expected they have the lowest potential. The simulation also gives current densities, represented as arrows coming out of the hull through anodes and get back through cathodes. Using equation (12) for the residual norm, results are obtained with a maximum error of 10^{-4} A/m² between injected and received currents.

2.3 Extrapolating the electromagnetic field

The previous step gives all the boundary conditions on the model, that is to say each $\partial\varphi/\partial n$ and φ at the elements barycenter. Physically, equivalence is possible between those results and virtual electrostatic sources in conduction problems. To deduct the electrical potential somewhere in the electrolyte, it is possible to use Green 3rd identity. The solid angle a Q point in the electrolyte see is -4π (the whole problem) so the equation becomes:

$$\begin{aligned} -4\pi\varphi(Q) &= \int_S \varphi(M) \cdot (\partial G(M, Q) / \partial n) dS \\ &- \int_S G(M, Q) \cdot (\partial \varphi(M) / \partial n) dS - 4\pi \cdot \varphi_\infty \end{aligned} \quad (17)$$

In this expression, the potential computed at the Q point will have the same offset than Fig. 5 due to the presence of the φ_∞ term. It is possible to remove this term to get the electric potential centered in zero. The boundary conditions are set with a point matching approximation, the values can be extracted from the integral terms and the meshing gives:

$$\begin{aligned} \varphi(Q) &= -\frac{1}{4\pi} \sum_{i=1}^N \frac{\partial \varphi(M_i)}{\partial n_i} \cdot \int_{\Omega_j} \frac{1}{r_{QM_i}} dS_{M_i} + \\ &\left(-\frac{1}{4\pi} \sum_{i=1}^N -\varphi(M_i) \cdot \int_{\Omega_j} \frac{\mathbf{n}_{M_i} \cdot \mathbf{r}_{QM_i}}{(r_{QM_i})^3} dS_{M_i} \right) \end{aligned} \quad (18)$$

Like the previous resolution, the first step will be to evaluate the integral terms and then use the boundary conditions to get the potential at point Q. Moreover the Maxwell Faraday gives the well known equation (1).

By using the opposite gradient of the potential calculation in (14), a new formula provides a simple electric field calculation:

$$\begin{aligned} \mathbf{E}(Q) &= \frac{1}{4\pi} \sum_{i=1}^N \frac{\partial \varphi(M_i)}{\partial n_i} \cdot \int_{\Omega_j} \frac{\mathbf{r}_{QM_i}}{(r_{QM_i})^3} dS_{M_i} \\ &+ \frac{1}{4\pi} \sum_{i=1}^N \left(-\varphi(M_i) \cdot \int_{\Omega_j} \left(\frac{3 \cdot \mathbf{r}_{QM_i} \cdot (\mathbf{r}_{QM_i} \cdot \mathbf{n}_{M_i})}{(r_{QM_i})^5} - \frac{\mathbf{n}_{M_i}}{(r_{QM_i})^3} \right) dS_{M_i} \right) \end{aligned} \quad (19)$$

Once again, from the boundary conditions on the model, it is possible to calculate the electric field with surface integrations. A result of electrical potential and field calculation is presented below on a grid under the model hull from the boundary conditions represented on Fig.6 (70*20 = 1400 square elements):

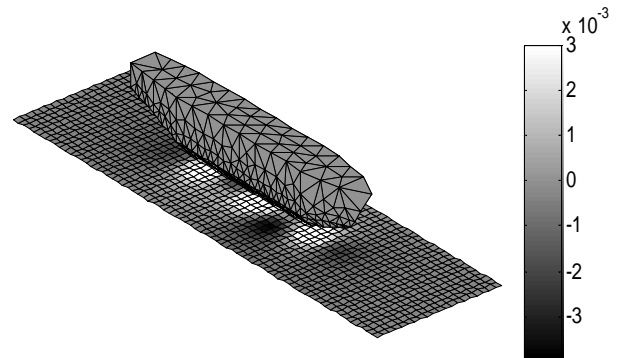


Fig. 7. Result of electric potential measurements made on the grid (1400 points) below the hull

The scale is still in volts, without caring about the infinite potential ($\varphi_\infty = 1.3762$ V). That is why the values are centered on zero. The field arrows are also represented but not well highlighted.

To get such results, a process can be imagined, like:

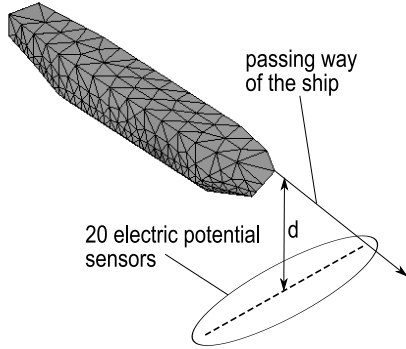


Fig. 8. Electric potential measurements principle: a ship passing over a series of 20 electric sensors at a determined depth, making 70 set of measurements. The final measurements number is then 1400.

3 DIAGNOSTIC: INVERSE METHOD

The purpose of this part is quite simple: the previous study provides a method which, from a set of boundary conditions of a defined geometry, predicts the electromagnetic field in the electrolyte. The inverse method consists in a boundary conditions reconstruction from a set of measurements. This method is often represented by the following simple equation:

$$A.X = B \quad (23)$$

B is a measurements vector, which can be electric or magnetic here. X is the unknown vector and A the interaction matrix between each measurement point and each unknown.

The main problem that appears in such methods is the condition number matrix A, directly linked to the difficulty to inverse it. Indeed matrix A does not often have the same number of rows and lines or contains values that are close to the computer zero (10^{-16}). These reasons give a bad condition number and, with a noisy B vector, lead to important difficulties to inverse the system (23). [6]

3.1 Naive inversion

Although matrix A has a bad condition number, it is possible to solve the normal equation to get a solution, which implies to find a minimum:

$$\min \|A.X = B\|_2 \quad (20)$$

This means to solve:

$$(A^t.A)X = A^t.B \quad (21)$$

This is possible by using a LU solver but some other exists. An example is developed hereinafter with the ship hull used before (N=1052 elements). Vector B is entirely described so the position of each barycenter of the grid is known. The A_{mes} matrix can be then easily built with (9) and (14). The unknown vector X will contain the potential and its normal derivative at the barycenter of each hull element (except for the anode (A in the further equations) whose current density is known).

This method only gives a mathematical convenient solution but often not physical. To focus these difficulties, an example Indeed vector B will first be simulated with the direct method. The 1400 electric potentials computed on a grid below the hull are taken adding 10% of the maximum potential random noise. This will be vector B. This induces a number of 2098 unknowns bringing the system under determined. In this case the system to inverse is:

$$[A_{mes}] \begin{bmatrix} \varphi_A \\ \varphi_{hull} \\ \frac{\partial \varphi_{hull}}{\partial n} \end{bmatrix} = [B - T_{mes} \cdot \frac{\partial \varphi_A}{\partial n}] \quad (22)$$

This is in the same form as (23). The results of a direct inversion are shown below:

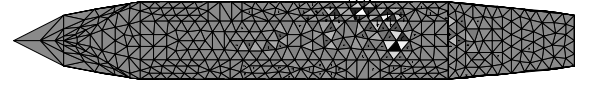
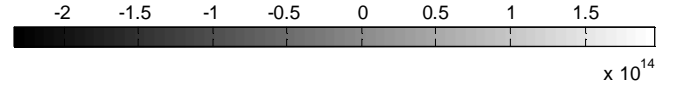


Fig. 9. Boundary conditions (electric potential and current densities) obtained on the hull with a “naive” inversion. The scale is in volts.

We obtain non physic boundary conditions with maximum potential values reaching 10^{14} (the target values are shown in Fig. 5). The first clue for the inversion problem is the bad condition number which is here equal to $4.1279 \cdot 10^{16}$. It is interesting to notice that the (23) equality is verified: the inversion is mathematically correct. The problem here is very ill-posed. A work on this system is necessary before inverting it to get a better solution.

One possible method would consist in 3 steps: first try to orthogonalize the system. Then an injection of additional information can make the system have a better condition number. Finally a regularization technique allows imposing a physical behavior to the solution [7]. The first step purpose, not described in this paper, is to change the basis description. The unknowns introduced (potential φ and its normal derivative) are representative of the physical phenomenon. There is no need to change them, as the other steps exposed before give good results.

3.2 Injection of information

The first step of pre conditioning is to add some information to the system. A smart way to do it is to use the straightforward matrix defined in (8) which links all unknowns of the inverse system. With the new meshing (no separation of cathodes and isolated parts), it becomes:

$$\begin{bmatrix} H_{11}+2\pi & H'_{12} & -4\pi & T_{11} & T'_{12} \\ H_{21} & H'_{22}+2\pi & -4\pi & T_{21} & T'_{22} \\ 0 & 0 & 0 & A_1 & A'_2 \end{bmatrix} \begin{bmatrix} \varphi_A \\ \varphi_{hull} \\ \varphi_{\infty} \\ \frac{\partial \varphi_A}{\partial n} \\ \frac{\partial \varphi_{hull}}{\partial n} \end{bmatrix} = [0] \quad (23)$$

diverging, which is main goal of an order zero regularization. An order 2 regularization with Green equations cumulates the two benefits.

The coefficient λ introduced is the regularization parameter, representative of the weight given to the regularization term $\|L.X\|$ in Tikhonov regularization. In the less noisy cases this term can have a very little value. On one hand, if a very high λ is taken, the solution is only regularized. On the other hand, if λ is very low, nothing changes from the previous solution (9).

Empirically, for a random noise reaching 10% of the maximal potential computed, λ is often chosen between 10^{-2} and 10^{-3} . If the λ term chosen has a value more than 5.10^{-1} , the solution obtained is often too smooth, erasing the discontinuity of the boundary conditions, which is mainly interesting here. Indeed the goal is to find the lowest potential areas, so that smoothing potential results makes the diagnosis inefficient. The regularization has then a too important influence. As a small conclusion, this parameter choice is the most important part of the inversion, because it is the only choice to do.

A good tool to choose a correct λ is the L-curve [9] which shows on a graph the solution semi norm $\|L.X\|$ toward the residual norm $\|A'.X - B'\|$ for different λ values. In the ship case, for a zero order regularization matrix, the L-curve obtained is shown below:

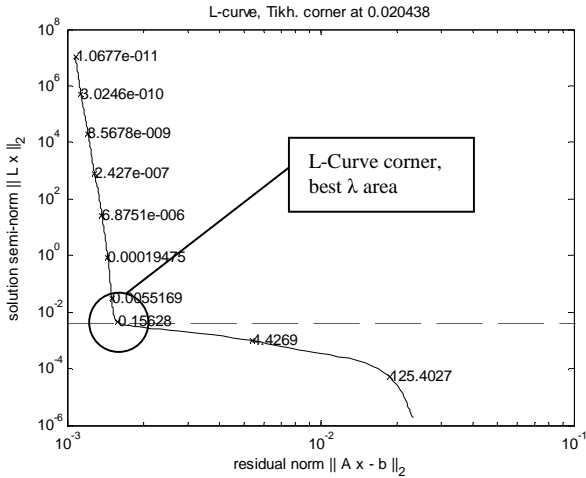


Fig. 11. L-Curve obtained for the considered problem. The highlighted corner points out the λ parameters giving the best compromise for the regularization.

This curve has often a corner which is the best area to choose the parameter. In this area, the solution semi norm and the residual norm have both values close to their minimum ones. It was the goal exposed before when introducing the problem in (31).

3.4 Final result and comparison with the target

When chosen, the inversion is possible, and the $\partial\varphi_{\text{hull}}/\partial n$ vector is obtained. As said above, the potential φ_A and φ_{hull} are then computed by forward modeling. The boundary conditions obtained on the hull are shown below:

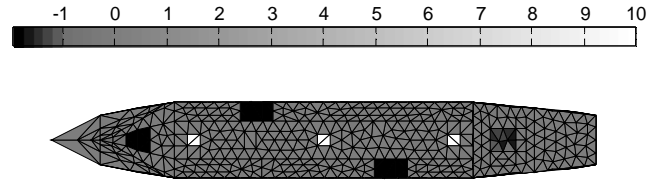


Fig. 12. Current densities obtained on the hull after inversion (scale in A/m^2)

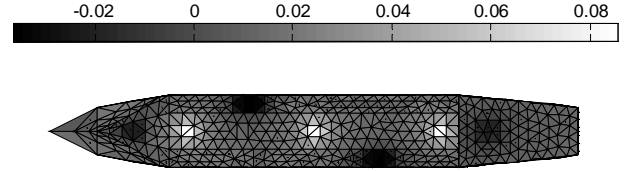


Fig. 13. Electric potentials computed on the hull with formula (12) (scale in Volts)

These results are very important because they give two boundary conditions which have to fit. Indeed corroded areas are situated where currents flow back into the hull, results got from the minimization of (32). As said above, potential on the hull are then obtained by forward modeling. The lowest ones are significant of a corroded area. The two previous figures show that the clues for corrosion are situated at the expected locations compared to the target on Fig.4 with the 1400 measurements. The diagnosis has well succeeded.

A last remark can be made about the measurements locations. It is obvious that measuring far away from reactions does not provide good results. But how guess the best locations? In the case presented here, the reactions are expected on the lowest parts of the hull; this is why the grid presented is placed below the hull. A better solution is to make measurements like a semi cylinder shape, to get more precisions on the sides of the hull. The other question is the maximum depth the measurements can reach to stay relevant. This needs a study on the seawater conductivity. The more conductive the electrolyte is, the closer the measurements have to be. Like any conduction problem, current lines spread more in a more resistive domain. A smart study is necessary before making any measurements.

The three steps (take well situated measurements, inject information and regularization) allow making a well corrosion diagnosis with noised measurements. For a clear visibility, the approach does not take the infinite potential into account, but it just can be added in (25). The next part deals with experimentations to check the results got with the presented algorithm.

4 EXPERIMENTATIONS

The previous parts have focused on an infinite problem, to fit with marine applications for example. Making directly a scale 1:1 experimentation would firstly face to memory consuming problems so that the first trial will be held in laboratory. The main idea is to reproduce a real case but at different scale, so that a one square meter PMMA bowls has been built with a 25cm depth. To fit the scale, the only thing to

do is to control the electrolyte salinity linked to the conductivity (in S.m).

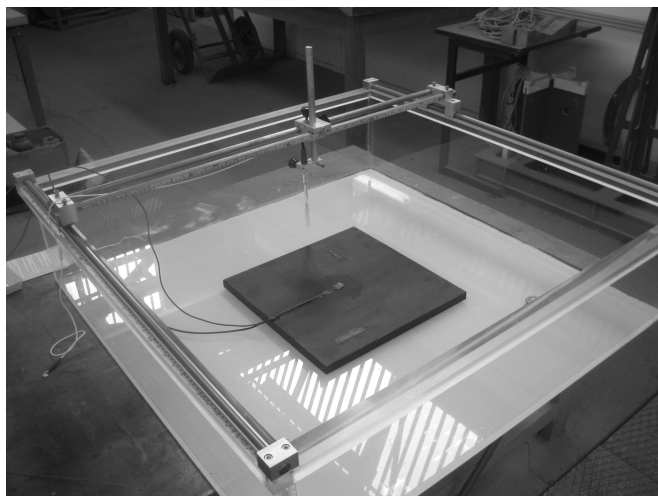


Fig. 14. PMMA bowl for first experimentations. The appropriate measurements system is also on the picture with a piece of protected steel in the middle.

A system of electrical potential measurements is held on the bowl: the principle is to measure electrochemical potentials in the electrolyte through a reference electrode (Calomel electrode) toward the iron potential. This can easily be with a multimeter whose positive side is connected to the reference electrode and the negative one directly to the iron in the electrolyte.

The model drawn in the bowl should be representative of the immersed part of a hull; it will be a piece of painted iron with paint defects (lack of paint) on it. To make this structure protected from corrosion, an ICCP is set on it with a platinum mesh (2x2 cm) set on its middle. The iron and platinum are electrically linked to a computer with adapted electrochemical equipment which can set and measure the current flowing into the electrolyte due to the platinum anode. The model meshed grid is shown below, with dimension 40x40x2 cm:

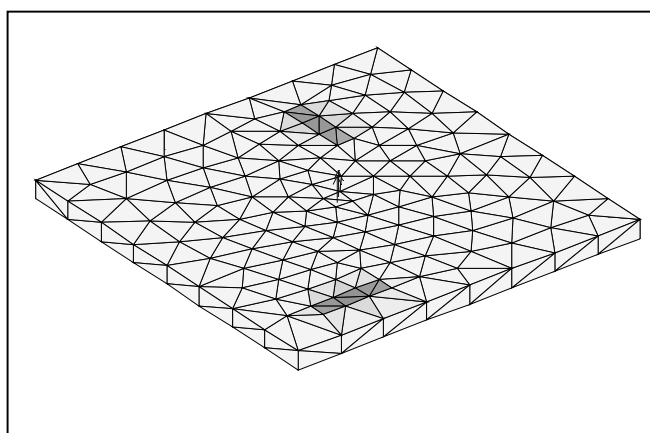


Fig. 15. Meshed model drawn in the bowl with 1 anode and two defects.

The anode in the middle is represented by the current densities it delivers with arrows. The two grey areas are the

defects with 8x4 cm dimension. The white areas are the well isolated part.

As the model geometry is well known, it can be drawn in the electrolyte. Seawater has conductivity close to 5.6 S.m, here it will be chosen equal to 0.1 S.m which is 56 times less. The current injected by the anode is 160 A/m² which makes 64 mA injected in the electrolyte. The reaction begins with a release of hydrogen on the iron and platinum. It needs to work on for a couple of hours depending on natural oxidation state of the iron. Then an electric potential measurement is made on a grid 2 cm above the model as shown:

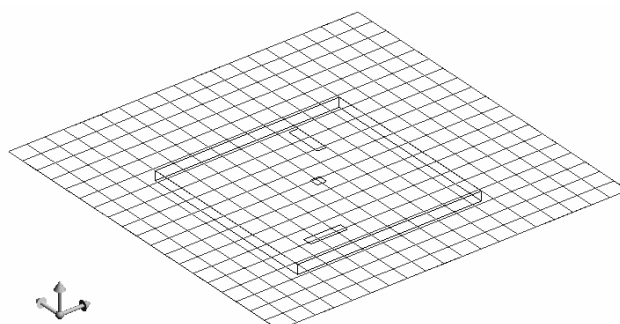


Fig. 16. Measurements locations set on a square grid above the piece of steel

Measurements are made at each barycenter of the grid; the bowl meshed representation has been set off for clarity.

The interaction matrix between measurement locations and the model is built, the Green equations are added and Tikhonov regularization is applied. The corresponding L-Curve is set below:

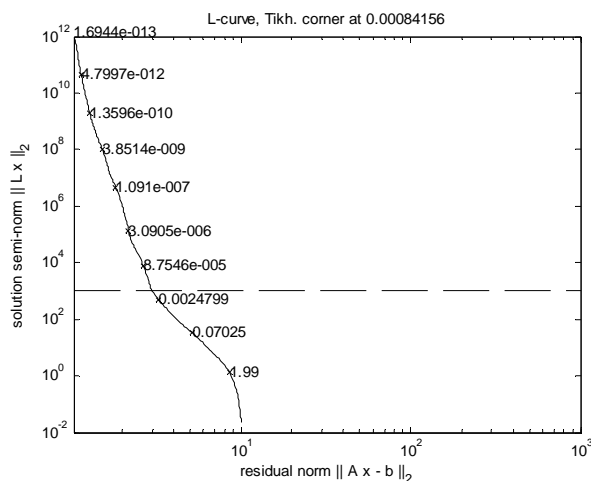


Fig. 17. Corresponding L-Curve of the system to inverse.

The corner is not as simple to see as in numerical cases. Indeed the problem comes from the salinity: to get a low conductivity (0.1 S.m), the salinity have to be very low. In the abacus, such salinities are subject to huge errors on the corresponding conductivity because of two main factors: the non homogenous temperature in the electrolyte and the salt purity (NaCl quantity in the salt) [10]. The information

injected with the known current density J_A through $\partial\phi_A/\partial n$ depends on the conductivity, so it induces errors on the inversion. The more noisy information the system has, the less significant the L-curve is. But the vertical dotted line gives us a clue of the inflection point. The λ parameter is taken equal to 0.0024 and the inversion gives the following electric potential results:

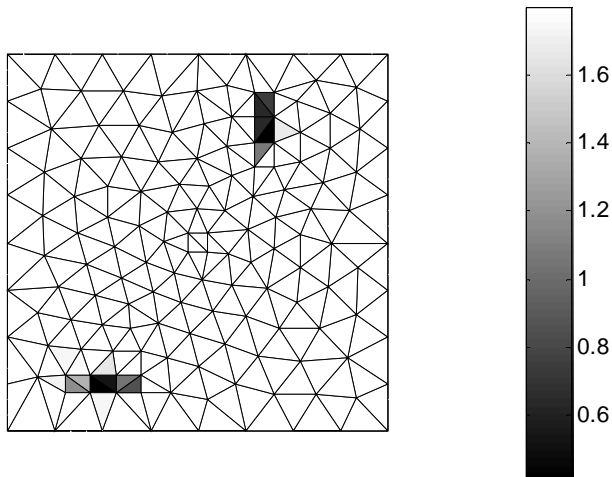


Fig. 18. Electric potential boundary conditions for a λ parameter equal to 0.0024 (scale in Volts)

To get visible results, only lowest potentials are represented. It is an arbitrary criterion: as the corroded areas have the lowest potential ones, it is decided that here only the 10% lowest ones are kept. The target is also calculated with the same criterion by forward modeling:

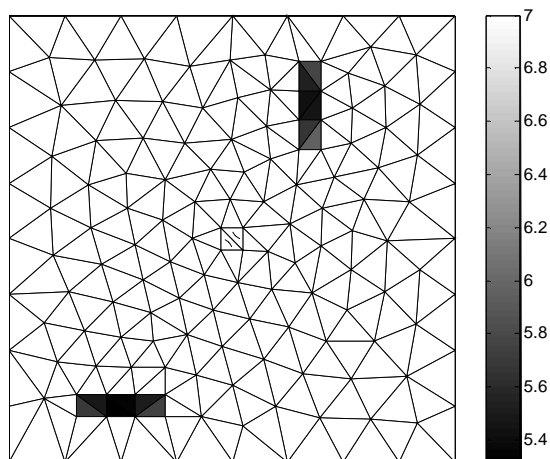


Fig. 19. Target of boundary conditions (electric potential) in the same conditions (scale in Volts)

The lowest potential areas are the same. The diagnosis is successful: the corroded areas have been explicitly recovered by the algorithm. The current density results give the same diagnosis and have not been exposed.

5 CONCLUSION

As a conclusion, the method explained in this article can be used in several domains such as ships hulls, oil platforms, underwater pipe lines, offshore wind energy platforms, etc... It can be also very useful to monitor water tanks, sewers pipes, silos, etc... Moreover other scientific topics such as thermal studies use the same equations and could take advantages of this method.

It provides a global tool to get clues about the state of an underwater iron structure with an appropriate cathodic protection. It must be said that this method works with internal or external problems with any cathodic protection (impressed current or sacrificial). An industrial application has been developed to examine the state of a hull at each passage in a harbor.

The next step of the approach is to constraint the inversion of the system by evaluation of the solution we want to find (current densities with order 2 regularization) or the permissible error due to measurement error prediction.

Other measurements have been made with scale 1:1 seawater (conductivity close to 5.6 S.m) in the bowl which works, but the current injection has obviously to be increased. Those results will be presented in further papers.

REFERENCES

- [1] J. Cheng, M. Choulli, X. Yang, "An iterative BEM for the inverse problem of detecting corrosion in a pipe", *Frontiers and Prospects of Contemporary Applied Mathematics* pp. 1-17, 2006.
- [2] R. Adey, J.M.W. Baynham, "*Predicting Corrosion Related Magnetics*", BEASY communication
- [3] C. A. Brebbia, J. C. F. Telles and L. C. Wrobel, *Boundary Elements Techniques, Theory and Applications in Engineering*, Springer-Verlag, Berlin, 1984.
- [4] N. G. Zamani, J. M. Chuang and J. F. Porter, "BEM simulation of cathodic protection systems employed in infinite electrolytes", *International Journal For Numerical Methods In Engineering*, vol. 24, pp. 605-620, 1987.
- [5] G. Dhatt, G. Touzot and E. Lefrançois, « Méthode des éléments finis », pp. 404-426, 2007.
- [6] J. Hadamard, "Lectures on Cauchy's Problem in Linear Partial Differential Equations", New Haven, Yale University, 1923.
- [7] O. Chadebec, J.L. Coulomb, J.P. Bongiraud, G. Cauffet, P. Le Thiec, "Recent improvements for solving inverse magnetostatic problem applied to thin hulls", *IEEE Trans. Magn.*, vol.38, pp.1005-1008, 2002.
- [8] A. N. Tikhonov and V. Y. Arsenine, *Solution of Ill-Posed Problem*. Washington, DC: Wiston/Wiley, 1977
- [9] C. Hansen, "Rank-Deficient and Discrete Ill-Posed Problems, Numerical Aspects of Linear Inversion", 1998
- [10] Keller, G.V., and Frischknecht, F.C., (1996) *Electrical methods in geophysical prospecting*, Pergamon, London.